

1 **Intergenerational transfer and sex differences of DNA methylation patterns in**
2 **the Pacific oyster (*Crassostrea gigas*)**

3
4 Yongguo Li^{1¶}, Wen Teng^{1¶}, Chengxun Xu¹, Hong Yu¹, Lingfeng Kong¹, Shikai Liu¹, Qi Li^{1,2*}

5
6 1 Key Laboratory of Mariculture, Ministry of Education, Ocean University of China, Qingdao
7 266003, China

8 2 Laboratory for Marine Fisheries Science and Food Production Processes, Qingdao National
9 Laboratory for Marine Science and Technology, Qingdao 266237, China

10

11 * Corresponding author

12 E-mail: qili66@ouc.edu.cn

13

14 ¶ These authors contributed equally to this work.

15

16 **Author Contributions**

17 Qi Li designed the experiment and reviewed the original draft. Yongguo Li and Wen Teng
18 analyzed the data and wrote the original draft. Chengxun Xu, Hong Yu, Lingfeng Kong, and Shikai
19 Liu contributed to the reagents/materials/analysis tools.

20

21 **Abstract**

22 Apart from DNA-sequence-based inheritance, inheritance of epigenetic marks such as DNA
23 methylation is controversial across the tree of life. In mammals, post-fertilization and primordial
24 germ cell reprogramming processes erased most parental DNA methylation information. In
25 nonmammalian vertebrates and insects, it has been proposed that DNA methylation is an essential
26 hereditary carrier. However, how and to what extent general DNA methylation reprogramming
27 affects intergenerational inheritance in molluscs remains unclear. Here, we investigated genome-
28 wide DNA methylation in a mollusc model, the Pacific oyster (*Crassostrea gigas*), to test how
29 epigenetic information transfers from parents to offspring. Analysis of global methylome revealed
30 that the DNA methylation patterns are highly conserved within families. Almost half of the
31 differentially methylated CpG dinucleotides (DMCs) between families in parents could transfer to
32 offspring. These results provided the direct evidence for the hypothesis that the Pacific oyster DNA
33 methylation patterns are inherited in generations. Moreover, distinct DNA methylation differences
34 between male and female somatic tissues in *C. gigas* are revealed in this study. These sex-
35 differential methylated genes significantly enriched in the regulation of Rho protein signal
36 transduction process, which indicated that DNA methylation might have an essential role in the
37 sexual differentiation of somatic tissues in *C. gigas*.

38 **Author Summary**

39 Transgenerational inheritance of DNA methylation marks varies across the tree of life. In
40 mammals, post-fertilization and primordial germ cell reprogramming processes obstructed the
41 DNA methylation transmission from parents to child, and only some CpG dinucleotides retain
42 gamete-inherited methylation. However, the DNA methylation inheritance seems apparent in

43 nonmammalian vertebrates and insects. As one of the essential mollusc models, the Pacific oyster
44 *Crassostrea gigas* have received the most substantial epigenetic studies, mainly focusing on the
45 DNA methylation profiles. While a previous study suggested the existence of paternal inheritance
46 of DNA methylation patterns in *C. gigas*, more data are needed to confirm this hypothesis. In this
47 study, genome-wide DNA methylation analysis was performed to investigate the epigenetic
48 inheritance in *C. gigas*. Almost half of the DNA methylation differences between families in
49 parents were found to be transferred to children, indicating the absence of global DNA methylation
50 reprogramming in *C. gigas*. Besides, extensive hypomethylation in *C. gigas* females compared
51 with males were also unveiled. These hypomethylated genes were significantly enriched in the
52 regulation of Rho protein signal transduction process. For example, guanine nucleotide exchange
53 factors, including *KALRN*, *FGDI*, and *FGD6*, were hypomethylated in *C. gigas* females, and the
54 corresponding transcriptions were significantly upregulated. Our findings provided insights into
55 the evolution of DNA methylation patterns, transgenerational epigenetic inheritance, and sexual
56 differentiation in molluscs.

57

58 **Introduction**

59 DNA methylation is a universal epigenetic regulatory mechanism found in prokaryotes and
60 eukaryotes [1, 2]. This prevalent epigenetic modification is essential for bacteria restriction-
61 modification (RM) systems [3] and mammal immune response [4], insect social behavior,
62 embryonic development [5], genome imprinting [6], inactivation of X-chromosome and tissue-
63 specific functions [7, 8]. In mammalian genomes, methylation usually occurs in CpG dinucleotides,
64 with more than 70% of CpG sites methylated [9]. Unlike the densely methylated genome in
65 vertebrates, genomic DNA methylation levels in invertebrates vary across taxa. In insects, Diptera

66 (fruit fly) nearly lost DNA methylation because of the absence of DNA methyltransferase
67 homologs. Hymenopteran (ants, bees, and wasps) had less than 4% DNA methylation levels, while
68 Blattodea had relatively higher levels of genomic DNA methylation, ranging from 1% to 14%
69 [10]. Similarly, cytosine methylation most occurs in CpG dinucleotides and the whole-genome
70 DNA methylation levels are highly variable in Molluscs ranging from 5 to ~15% [11].

71 Genetic information provides the primary substrate of inheritable traits across generations.
72 Apart from the DNA sequence-based inheritances, many phenomena of epigenetic-based
73 inheritances, including DNA methylation, histone modification, and small non-coding RNAs, have
74 been reported in organisms [12, 13]. In mammals, genome-wide DNA methylation traits
75 experienced erasure and establishment twice: first after the fertilization and second during the germ
76 cell formation [5]. Two waves of DNA methylation reprogramming are the obstruction of DNA
77 methylation inheritance. Only a small number of parentally imprinted genes escaped
78 reprogramming in the early development of the embryo [14, 15]. However, nonmammalian
79 vertebrates do not undergo genome-wide DNA methylation reprogramming during embryogenesis
80 [16]. For example, zebrafish retained the paternal epigenetic memory in primordial germ cells
81 (PGC) in stark contrast to the findings in mammals [17, 18]. In invertebrates, limited studies give
82 details of the DNA methylation remodeling and epigenetic inheritance. Recent investigations
83 revealed that DNA methylation reprogramming during embryogenesis was absent in cnidarians
84 and protostomes such as insects [16]. For instance, honey bees are reported to have highly
85 conserved DNA methylation patterns between generations [19]. Stable inheritance of an epigenetic
86 signal in *Nasonia* was also found in F₁ hybrids [20]. These results suggested that the DNA
87 methylation reprogramming seems to be a mammalian-specific feature [19].

88 As a typical Mollusc model species, the Pacific oyster *Crassostrea gigas* has moderate
89 genomic DNA methylation levels in CpG dinucleotides, ranging from 12 to 18% due to sampling
90 status and methylation calling methods in various studies. Because of the ecological and economic
91 values, *C. gigas* has the most extensive DNA methylation studies in Molluscs [11]. These works
92 are primarily concerned with gene expression regulation [21-23], development processes [24, 25],
93 phylotypic plasticity [26, 27]. While the previous study hypothesized that intergenerational
94 inheritance in DNA methylation exists in *C. gigas* [25], more evidence is needed to make general
95 conclusions. Moreover, among most of the epigenetic studies in *C. gigas*, the sex differences in
96 somatic tissues were neglected. One reason is the difficulty in gender determination out of
97 spawning season. The other reason is underestimated genome-wide DNA methylation differences
98 between male and female somatic tissues in *C. gigas*.

99 Here, we produced diploid and triploid Pacific oysters in two independent families. Whole-
100 genome bisulfite sequencing (WGBS) of both parent and offspring muscle tissues were then
101 performed in each family to investigate the epigenetic inheritance, sexual differences, and effects
102 of chromosome ploidy in DNA methylation in *C. gigas*. We wish our work could add one more
103 puzzle piece to the image of epigenetic studies in Molluscs.

104

105 **Results**

106 **Globally DNA methylation landscape of *C. gigas***

107 To profile the inheritance patterns of DNA methylation in *C. gigas*, regular F₁ diploid and
108 triploid oysters were produced by crossing a normal diploid male and female oysters in two
109 independent families. The whole-genome bisulfite sequencing (WGBS) was then performed using
110 muscle tissues from both parents, three diploid and three triploid offspring individuals in each

111 family. RNA sequencing (RNA-seq) was also introduced to profile the transcription in the same
112 muscle tissues in offspring (S1A Fig). In total, an average of 66.8 million 150 pair-end reads
113 covering 9 million CpGs (> 68% of the total CpG sites) at least five times were obtained in each
114 sample (S1 Table). DNA methylation ratio was relatively consistent with increasing read depth,
115 which excluded the sequencing depth-induced bias in methylation calling (S1B Fig). Bisulfite
116 conversion efficiencies reached 99.9% in all analyzed samples. The average DNA methylation
117 levels ranged from 0.11 to 0.14 (Fig 1A), consistent with previous studies [26, 27]. Compared with
118 public WGBS data of *C. gigas* [21, 22, 26, 27], high Pearson correlation coefficients (average $r =$
119 0.858) were found between our sequencing data and public datasets (S1C Fig). In all, the WGBS
120 data quality in this study is solid.

121 Next, the *C. gigas* DNA methylation profile was compared with that of two other bivalve
122 model organisms, *Crassostrea virginica* [28] and *Patinopecten yessoensis* [26], to investigate the
123 conserved and derived DNA methylation patterns in bivalves. Under the same data analysis criteria,
124 the average DNA methylation level of *C. gigas* (mCG/CG = 0.12) was consistent with that of *C.*
125 *virginica* (mCG/CG = 0.12) but relatively lower than *P. yessoensis* (mCG/CG = 0.17). The
126 frequency of DNA methylation ratios of *C. gigas*, *C. virginica*, and *P. yessoensis* displayed a non-
127 classical bimodal distribution with a major peak at 0 (unmethylated) and a minor peak at 1 (fully
128 methylated), which is distinct from that of vertebrates (Fig 1B and S1D Fig). However,
129 hypermethylated gene body and hypomethylated transcriptional start sites (Fig 1C and S1E Fig)
130 are like other eukaryotes [29]. To further claim the DNA methylation patterns in bivalves, we
131 compared the DNA methylation levels within various regulatory elements. We observed
132 consistently high methylation levels in bivalve genomic regions, including exon, intron, simple
133 repeats, and DNA transposons, but low methylation in CpG islands (CGIs), promoters, long

134 interspersed nuclear elements (LINEs), and long terminal repeats (LTRs). Despite these
135 consistencies, there were low DNA methylation levels within rolling-circle transposons but
136 relatively high DNA methylation levels in low complexity repeats and short interspersed nuclear
137 elements (SINEs) in *C. gigas* (Fig 1D and S1F Fig).

138 The function of DNA methylation to repress transcription has long been recognized [30]. In
139 *C. gigas*, TSS regions remained almost absent of DNA methylation in both active and inactive
140 genes and showed no strict linear inverse relationship with the transcription (Fig 1E and S1G Fig).
141 The gene body methylation plateau is reported to exhibit a parabolic relationship with transcription:
142 moderately expressed genes are most likely to be methylated, whereas the most active and non-
143 active genes have lower methylation levels [21, 26]. However, our data showed that gene body
144 methylation in both diploid and triploid oysters had a linear relationship with gene expression (Fig
145 1E and S1G Fig).

146

147 **Fig 1. DNA methylation profiles of *C. gigas* muscle tissues**

148 (A) Global DNA methylation levels (quantified as mean mCG/CG) of oysters ranged from 0.11 to
149 0.14. (B) Histograms of DNA methylation levels distributions for human (*Homo sapiens*) muscle
150 cells, zebrafish (*Danio rerio*) muscle cells, Yesso scallop (*Patinopecten yessoensis*) mantle tissues,
151 eastern oyster (*Crassostrea virginica*) reproductive tissues, and the Pacific oyster (*C. gigas*)
152 muscle tissues in this study. (C) DNA methylation levels across the gene body in *C. gigas*, *C.*
153 *virginica*, and *P. yessoensis*. (D) DNA methylation levels at the indicated regulatory elements in
154 *C. gigas*, *C. virginica*, and *P. yessoensis*. (E) The relationship between DNA methylation levels
155 and transcripts across the gene body.

156

157 **DNA methylation inheritance and sex-specific DNA methylation differences in *C. gigas***

158 The gender of parent cohort was determined by checking germ cells during the breeding
159 process. Because progenies were out of sexual maturity stages, offspring samples were sexed by
160 DNA methylation markers at the diacylglycerol kinase delta (*DGKD*) locus, which was
161 hypermethylated in males and hypomethylated in females [31]. The DNA methylation marker was
162 reconfirmed in parent groups and public data (S2A Fig). All triploid and two diploid samples were
163 found to be females, while the other four diploid oysters were males (S2B Fig and S2 Table).

164 Next, we compared the methylation density using all sample shared CpGs in each colony
165 (excluded common CpGs with zero methylation level in all specimens) to test whether there were
166 global changes of DNA methylation between generations and different genders. Overall, parents
167 and progenies had similar methylation densities, but female DNA methylation levels were found
168 to be lower than males ($P < 0.00001$; Fig 2A). These hypomethylation patterns in females spread
169 across chromosomes and enriched in genomic region including exon, intron, and low complexity
170 regions (S2C Fig). Unsupervised hierarchical clustering analysis based on the top 10,000 variable
171 common CpGs across all samples distinguished females from male groups. Under the main
172 clusters of different genders, samples from colony one constituted a distinct sub-cluster, separated
173 from colony two (Fig 2B). These findings revealed distinct global DNA methylation differences
174 across genders and families in *C. gigas*.

175 To confirm these findings, Pearson correlation analysis was performed using pairwise
176 common CpGs across all samples analyzed in this study. There were relatively high Pearson
177 correlation coefficients among samples in two main clusters (male and female clusters) and even
178 higher Pearson correlation coefficients among samples in colony subclusters (S2B Fig). Principal
179 component analysis using all sample shared CpGs, including 5.9 million CpG dinucleotides was

180 also conducted. The principal component one divided all individuals into male and female groups.
181 Meanwhile, the principal component two divided all samples into two colony groups (Fig 2C).

182 To evaluate whether differences between colonies, male and female groups in parents were
183 recapitulated in offspring. We identified differentially methylated cytosines (DMCs) by comparing
184 colony one and colony two, male and female groups in parents and offspring using MOABS [32],
185 respectively. In progenies, we found a great deal of DMCs between colonies, male and female
186 groups, but much fewer DMCs between diploid and triploid groups (S2C Fig). These results
187 reconfirmed that there are no global DNA methylation differences between diploid and triploid
188 oysters [33]. Furthermore, we found almost half of the DMCs, including hypo-DMCs and hyper-
189 DMCs, between colony one and colony two in parents transferred to offspring (Fig 2D). Moreover,
190 female groups in offspring displayed a global decrease in DNA methylation, consistent with that
191 of parents (S2E Fig). And a great deal of hypo-DMCs between males and females in parent cohorts
192 were recapitulated in offspring (Fig 2E).

193 Overall, our results indicated that there is no DNA methylation reprogramming in *C. gigas*,
194 and almost half of the family-specific DNA methylation marks could be stably transferred between
195 generations. Besides, sexual differentiation in DNA methylation profiles exist in *C. gigas* somatic
196 tissues.

197

198 **Fig 2. Inheritance and sex differences of DNA methylation in *C. gigas* muscle tissues**

199 (A) DNA methylation levels across samples in colony one (left) and two (right). Violin plots
200 represent kernel density plot. Boxplots represent median and interquartile range. (B) Heatmap of
201 DNA methylation levels using the top 10,000 variable common CpGs across all samples in this
202 study. (C) Principal component analysis (PCA) of DNA methylation levels in shared CpGs across

203 all samples in this study. (D) UpSet plots showing the integrated comparative analysis of hypo-
204 DMCs (left) and hyper-DMCs (right) between parents and offspring. DMCs are identified between
205 colonies. (E) UpSet plots showing the integrated comparative analysis of hypo-DMCs (left) and
206 hyper-DMCs (right) between parents and offspring. DMCs are identified between males and
207 females.

208

209 **Activation of Rho signaling in *C. gigas* females**

210 To investigate DNA methylation differences between males and females in *C. gigas* muscle
211 tissues, the differentially methylated regions (DMRs) were identified by comparing the male and
212 female groups in parents and offspring, respectively. In consequence, 10,180 hypo-DMRs and
213 3,555 hyper-DMRs were found in parent cohort. Similarly, 9,794 hypo-DMRs and 196 hyper-
214 DMRs were found in offspring cohort (Fig 3A). Across generations, 4,148 hypo-DMRs and 23
215 hyper-DMRs were shared by parent and offspring cohorts (Fig 3B), which suggested a stable
216 decrease of DNA methylation in females in *C. gigas* muscle tissues. These stably inherited hypo-
217 DMRs in females scattered across all chromosomes and mainly enriched in gene bodies, especially
218 in intron regions (S3A and B Fig). AgriGO v2.0 [34] was then used to perform gene ontology
219 (GO) enrichment analyses. We found these common hypo-DMR related genes are highly enriched
220 in the regulation of Ras homology (Rho) protein signal transduction process (Fig 2C and S3C Fig).
221 The Rho GTPases switch cycled between the inactive (GDP-bound) and active (GTP-bound)
222 forms, regulated by guanine nucleotide exchange factors (GEFs) and GTPase-activating proteins
223 (GAPs) (Fig 3D). Active GTP-bound GTPases interact with various downstream effectors and
224 regulate a wide range of cellular responses [35]. In this study, 21 genes function as GEFs were
225 found to be hypomethylated in females compared to males (S3 Table). For example, the DNA

226 methylation levels at *KALRN*, *FGDI*, and *FGD6* locus were significantly decreased in females
227 compared with that in males in *C. gigas* (Fig 3E and S3D Fig). Hypomethylation consequently
228 promoted the gene expression as the transcriptions of *KALRN*, *FGDI*, and *FGD6* of females were
229 significantly higher than that of males in *C. gigas* (Fig 3F and S3E Fig).

230 These results suggested that epigenetic differences exist between males and females in *C.*
231 *gigas* muscle cells, and the DNA methylation signature at GEFs genes can be used as biomarkers
232 to distinguish the gender of *C. gigas*. Besides, these intrinsic epigenetic differences in the Rho
233 protein signal transduction process may contribute to sex-dependent differences in *C. gigas* muscle
234 phenotypes.

235

236 **Fig 3. Functional annotation of cytosine methylation differences between male and female in**
237 ***C. gigas***

238 (A) Histogram showing the numbers of hypo-DMRs and hyper DMRs identified between males
239 and females in parent groups and offspring groups. (B) UpSet plots showing the integrated
240 comparative analysis of hypo-DMRs (left) and hyper-DMRs (right) between parents and offspring.
241 DMRs are identified between males and females in *C. gigas*. (C) Gene ontology (GO) enrichment
242 analysis for shared hypo-DMRs related genes across parent and offspring cohorts. Hypo-DMRs
243 are identified between males and females in *C. gigas*. The x-axis shows the false discover rate
244 (FDR) value. (D) Overview of Rho GTPase regulation. (E) UCSC genome browser view of DNA
245 methylation enrichment at the *KALRN* locus (NC_047565.1:11384273-11464307) in all samples
246 analyzed in this study. The highlighted region by dotted line exhibits decreased methylation in
247 females. (F) Boxplot showing the FPKM values in male and female groups in offspring ($P < 0.01$).
248

249 **Discussion**

250 DNA methylation is prevalent in eukaryotic organisms [36]. This epigenetic modification
251 mechanism is especially predominant in vertebrates but varies greatly in invertebrates. In bivalves,
252 the global DNA methylation levels of CpG dinucleotides have been shown conventional
253 invertebrate-like patterns with a majority CpGs unmethylation [11]. However, the unmethylated
254 CpG islands and apparent gene-body methylation in bivalves were like that of other eukaryotic
255 organisms; these conserved methylation patterns may serve as an ancient feature through the
256 evolution of eukaryotes [29, 37]. In oyster and scallop genomes, we found apparent DNA
257 methylation in some repetitive elements, including simple repeat and DNA transposon. In contrast,
258 the methylation of some retrotransposons, including LTR and LINE, occurs only at moderate
259 levels. Despite these consistencies, differences in cytosine methylation also exist within bivalve
260 species. For example, the global cytosine methylation in scallops is higher than in oysters. *C. gigas*
261 also showed some species-specific methylation patterns. The rolling-circle transposable elements,
262 *helitrons*, in *C. gigas* displayed a moderate methylation level. *Helitrons* amplified significantly in
263 *C. gigas* genome and were proposed to be remnants of the past activity of evolution [38]. The
264 diminish of cytosine methylation in *Helitrons* may also be the result of ancient activations, as
265 deamination is often needed for transposable elements to take on regulatory functions [39].

266 The repressive effect of DNA methylation at promoters on transcription initiation has long
267 been recognized [30]. High methylation levels at promoters may exclude the DNA-binding factors
268 and consequently depress the transcription [40]. However, gene body methylation is positively
269 correlated with gene expression [41, 42]. It was proposed that the DNA methylation in the gene
270 body facilitates the transcription elongation and affects splicing [43, 44], and that it inhibits
271 intragenic promoters [45]. In *C. gigas*, DNA methylation is predominantly enriched in intragenic

272 regions, especially in exon. Similarly, this gene-body methylation is positively correlated with
273 transcriptions. These conservative patterns and functions indicated the fundamental roles of DNA
274 methylation in *C. gigas*.

275 The absence of DNA reprogramming has been observed in cnidarians and protostomes [16].
276 For example, DNA methylation marks are stably transferred between generations in honey bees
277 [19]. Besides, a previously underestimated fraction of the vertebrate genome could even bypass
278 the DNA methylation reprogramming process [13, 46]. However, the epigenetic inheritance in
279 molluscs remains poorly understood. A previous study had suggested that DNA methylation
280 patterns are inherited in *C. gigas* [25], but direct evidence for this hypothesis was no longer
281 provided. Our data corroborated that almost half of the methylation differences between colonies
282 in parents could transfer to the next generations. The stable DNA methylation inheritance in *C.*
283 *gigas* provides the basis to study the environmentally induced epigenetic changes and inheritance.

284 DNA methylation has been reported to differ males and females in mammalian tissues,
285 including islets [47], brain [48], and skeletal muscle [49]. However, most mollusc studies
286 neglected these differences between genders, especially in *C. gigas*. Researchers consistently
287 underestimated the differences between males and females in *C. gigas* somatic tissues. In this study,
288 distinct DNA methylation profiles between male and female muscle tissues were unveiled in *C.*
289 *gigas* (Fig 3A and B). These epigenetic differences (DMRs) are not enriched in solo chromosomes
290 but scattered across the genome (S3A Fig). Besides, the DMRs between males and females are
291 enriched in genetic regions, especially in intro regions, indicating the potential genetic regulation
292 roles of the methylation alteration. Gene ontology analyses revealed significant enrichment for the
293 regulation of Rho protein signal transduction process across the differentially methylated genes.
294 Specifically, 21 GEFs genes activating the GTPase by exchanging bound GDP for free GTP were

295 hypomethylation in females. The transcription of three GEFs, including *KALRN*, *FGDI*, and
296 *FGD6*, were also found upregulated in females compared with males. Rho GTPases are highly
297 conserved across all eukaryotes and are best known for their roles in several cellular processes,
298 including cytoskeletal organization, cell cycle progression, apoptosis, and membrane traffic [35].
299 Previous studies have shown Rho GTPases have a critical role in human muscle development,
300 regeneration, and function [50, 51]. The distinct nucleotide methylation differences at these GEFs
301 locus between *C. gigas* males and females indicated that Rho GTPase signaling might contribute
302 to the muscular phenotypes. Therefore, we highly recommend taking gender into consideration in
303 epigenetic studies in *C. gigas*.

304 DNA methylation is an essential epigenetic modification mechanism, and it has long been
305 shown involved in *C. gigas* gene expression, embryonic development, growth, sex differentiation,
306 genetic inheritance, and phenotype plasticity. This study emphasized the influences of DNA
307 methylation marks in genetic inheritance and sexual differentiation in somatic tissue developments
308 in *C. gigas*. But so far, we still lack large pieces of the entire DNA methylation landscapes of *C.*
309 *gigas*. For example, tissue-specific DNA methylation patterns, gametogenesis and embryo
310 development DNA methylation dynamics at base resolution are poorly understood. Future work
311 towards these basic epigenetic studies in *C. gigas* is required.

312

313 **Conclusion**

314 The present work provided direct evidence that DNA methylation patterns could transfer
315 between generations. We hypothesises that there is no global DNA methylation reprogramming in
316 *C. gigas*. Distinct DNA methylation differences exist between male and female oyster somatic
317 tissues. The CpG dinucleotides alteration in Rho GTPases cycle may control the sex-based

318 differences in muscular phenotypes. Specifically, hypomethylation in GEFs in *C. gigas* females
319 activates the Rho GTPases switch and activates the downstream factors. These findings provide
320 new insights into the DNA methylation influences in genetic inheritance and sexual
321 differentiation in molluscs.

322

323 **Materials and methods**

324 **Animals**

325 One normal diploid male and female oysters were selected for mating from two full-sib
326 families, respectively. In each family, fertilized eggs were divided into two equal groups. One
327 group was treated with cytochalasin B (CB, 0.5 mg L⁻¹) for 15 min once 50 % of the eggs released
328 the first polar body to produce the triploid oysters. The other untreated group produced diploid
329 oysters normally. Progenies were reared separately for one year. Chromosome ploidy of each
330 sample was determined using flow cytometry to check the whole genome DNA contents stained
331 by DAPI. In each family, adductor muscles from male and female parents, three diploid progenies,
332 and three triploid progenies were frozen by liquid nitrogen and then transferred to a -80 °C
333 refrigerator for long-term preservation.

334

335 **WGBS library construction and data analysis**

336 Genomic DNA (gDNA) was isolated from adductor muscle tissues in parents and offspring
337 using the TIANamp Marine Animals DNA Kit (TIANGEN, Beijing). Library preparation and
338 high-throughput sequencing were conducted by Novogene (Beijing, China). Briefly,
339 approximately 5.2 µg of purified gDNA (spiked with 1% unmethylated lambda DNA, Promega)
340 was sheared into fragment size of 200-300 bp using Covaris S220. These DNA fragments were

341 then subjected to bisulfite conversion using EZ DNA Methylation-Gold™ Kit (Zymo Research).
342 The resulting bisulfite-converted DNA fragments were amplified by PCR and then purified by
343 AMPure XP beads (Beckman Coulter). Finally, the library was sequenced on Illumina HiSeq
344 platform with cBot System via TruSeq PE (Paired-End) Cluster Kit v3-cBot-HS (Illumina, US).
345 For WGBS data analysis, raw FASTQ data were filtered using *fastp* v.0.20.1 [52] with main
346 parameters (--cut_front --cut_front_window_size=1 --cut_front_mean_quality=3 --cut_tail --
347 cut_tail_window_size=1 --cut_tail_mean_quality=3 --cut_right --cut_right_window_size=4 --
348 cut_right_mean_quality=15 --trim_front1 10 --trim_front2 10). The filtered FASTQ files were
349 then mapped to *C. gigas* reference genome (GCF_902806644.1) using bsmap v.2.90 [53] with
350 parameters (-R -p 4 -n 1 -r 0 -v 0.1 -S 1). BSeQC [54] were used to evaluate the quality of bisulfite
351 sequencing output. The CpG coverage and DNA methylation calling were performed using
352 MCALL module in MOABS v.1.3.0 [32]. In this study, only CpG sites sequenced by at least 5
353 times were retain in the following analysis. Bisulfite conversion efficiency was estimated by spike-
354 in unmethylated lambda DNA. The significant differentially methylated CpG sites (DMCs) and
355 differentially methylated regions (DMRs) were identified using MCOMP module in MOABS with
356 main parameter (--withVariance 1). Bigwig files were upload to UCSC genome browser for
357 visualization. Functional annotations were performed using AgriGO v2.0 [34].

358

359 **mRNA-seq library construction and data analysis**

360 Total RNA was isolated from muscle tissues in offspring using RNAprep Pure Tissue Kit
361 (TIANGEN, Beijing). According to the manufacturer's instructions, library constructions were
362 performed using TruSeq Stranded mRNA LT Sample Prep Kit (Illumina, US). In brief, samples
363 with the RNA integrity number (RIN) ≥ 7 were used in the following two rounds of mRNA

364 purification using oligo-dT beads to capture polyA tails. RNA fragmentations were performed by
365 Covaris S220. Then the first strand cDNA was synthesized by reverse transcribing the cleaved
366 RNA fragments primed with random primer. Second strand cDNA was synthesized via
367 incorporating dUTP in place of dTTP, and the dUTP strand degraded in the following
368 amplification process. One adenine nucleotide was added to the 3' ends of blunt fragments. Finally,
369 indexing adapters were ligated to the ends of the double-strand cDNA fragments. Each library was
370 deeply sequenced on Illumina NovaSeq 6000.

371 For RNA-seq data analysis, raw FASTQ data was filtered using *fastp* v.0.20.1 as previously
372 described. The filtered FASTQ files were then mapped to *C. gigas* reference genome
373 (GCF_902806644.1) using HISAT2 v.2.2.1 [55]. Mapped reads with mapping quality ≥ 30 were
374 retained in the following analysis. Read counts and FPKM was calculated using HTSeq 2.0 [56].

375

376 **Public data**

377 Public WGBS data of 22 *C. gigas* samples were downloaded from PRJNA213124,
378 PRJNA173440, PRJNA562805, and PRJNA689936. WGBS data of four *H. sapiens* samples were
379 downloaded from PRJNA63443. WGBS data of four *D. rerio* samples were downloaded from
380 PRJNA553572 and PRJNA628650. WGBS data of six *P. yessoensis* samples were downloaded
381 from PRJNA695315. Reduced representation bisulfite sequencing (RRBS) data of 77 *C. virginica*
382 samples were downloaded from PRJNA488288.

383 All public data were analyzed under the same criteria as described above. *H. sapiens* reads
384 were mapped to NCBI Human Reference Genome Build GRCh38 (hg38). *D. rerio* reads were
385 mapped to GCF_000002035.6 (GRCz11). *P. yessoensis* reads were mapped to GCF_002113885.1
386 (ASM211388v2). *C. virginica* reads were mapped to GCF_002022765.2 (C_virginica-3.0).

387 Considering the low coverage of RRBS data of *C. virginica*, we merged all data into one sample.
388 Transposable element files of *H. sapiens* and *D. rerio* were downloaded from NCBI. Putative
389 transposable elements of *P. yessoensis*, *C. virginica*, and *C. gigas* were identified with
390 RepeatMasker v4.1.2 [57] using the mollusca RepBase repeat library [58] and RepeatModeler [59].

391

392 **Data availability**

393 WGBS and RNA-seq data are available at the NCBI under the project number PRJNA801419.
394 All relevant data supporting our findings are available within the article and supplementary
395 information files or from the corresponding author for reasonable request.

396

397 **Acknowledgments**

398 This work was supported by the China Agriculture Research System Project (CARS-49), and
399 Earmarked Fund for Agriculture Seed Improvement Project of Shandong Province
400 (2020LZGC016).

401

402 **Reference**

- 403 1. Sánchez-Romero MA, Casadesús J. The bacterial epigenome. *Nature Reviews Microbiology*.
404 2020;18(1):7-20. pmid: 31728064
- 405 2. Zemach A, McDaniel IE, Silva P, Zilberman D. Genome-wide evolutionary analysis of
406 eukaryotic DNA methylation. *Science*. 2010;328(5980):916-9. pmid: 20395474.
- 407 3. Blow MJ, Clark TA, Daum CG, Deutschbauer AM, Fomenkov A, Fries R, et al. The epigenomic
408 landscape of prokaryotes. *PLoS genetics*. 2016;12(2):e1005854. pmid: 26870957

- 409 4. Pingoud A, Wilson GG, Wende W. Type II restriction endonucleases--a historical perspective
410 and more. *Nucleic acids research*. 2014;42(12):7489-527. pmid: 24878924
- 411 5. Greenberg MVC, Bourc'his D. The diverse roles of DNA methylation in mammalian
412 development and disease. *Nature Reviews Molecular Cell Biology*. 2019;20(10):590-607. pmid:
413 31399642
- 414 6. Xie W, Barr Cathy L, Kim A, Yue F, Lee Ah Y, Eubanks J, et al. Base-Resolution Analyses of
415 Sequence and Parent-of-Origin Dependent DNA Methylation in the Mouse Genome. *Cell*.
416 2012;148(4):816-31. pmid: 22341451
- 417 7. Riggs AD, Pfeifer GP. X-chromosome inactivation and cell memory. *Trends in Genetics*.
418 1992;8(5):169-74. pmid: 1369742
- 419 8. Schultz MD, He Y, Whitaker JW, Hariharan M, Mukamel EA, Leung D, et al. Human body
420 epigenome maps reveal noncanonical DNA methylation variation. *Nature*.
421 2015;523(7559):212-6. pmid: 26030523
- 422 9. Bird A. DNA methylation patterns and epigenetic memory. *Genes & development*.
423 2002;16(1):6-21. pmid: 11782440
- 424 10. Goll MG, Bestor TH. Eukaryotic cytosine methyltransferases. *Annu Rev Biochem*.
425 2005;74:481-514. pmid: 15952895
- 426 11. Fallet M, Luquet E, David P, Cosseau C. Epigenetic inheritance and intergenerational effects
427 in mollusks. *Gene*. 2020;729:144166. pmid: 31678264
- 428 12. Miska EA, Ferguson-Smith AC. Transgenerational inheritance: Models and mechanisms of
429 non-DNA sequence-based inheritance. *Science*. 2016;354(6308):59-63. pmid: 27846492
- 430 13. Skvortsova K, Iovino N, Bogdanović O. Functions and mechanisms of epigenetic inheritance
431 in animals. *Nature Reviews Molecular Cell Biology*. 2018;19(12):774-90. pmid: 30425324

- 432 14. DeChiara TM, Robertson EJ, Efstratiadis A. Parental imprinting of the mouse insulin-like
433 growth factor II gene. *Cell*. 1991;64(4):849-59. pmid: 1997210
- 434 15. Ferguson-Smith AC. Genomic imprinting: the emergence of an epigenetic paradigm. *Nature*
435 *Reviews Genetics*. 2011;12(8):565-75. pmid: 21765458
- 436 16. Xu X, Li G, Li C, Zhang J, Wang Q, Simmons DK, et al. Evolutionary transition between
437 invertebrates and vertebrates via methylation reprogramming in embryogenesis. *National*
438 *Science Review*. 2019;6(5):993-1003. pmid: 34691960
- 439 17. Ortega-Recalde O, Day RC, Gemmell NJ, Hore TA. Zebrafish preserve global germline DNA
440 methylation while sex-linked rDNA is amplified and demethylated during feminisation. *Nature*
441 *communications*. 2019;10(1):1-10. pmid: 31311924
- 442 18. Skvortsova K, Tarbashevich K, Stehling M, Lister R, Irimia M, Raz E, et al. Retention of
443 paternal DNA methylome in the developing zebrafish germline. *Nature communications*.
444 2019;10(1):1-13. pmid: 31296860
- 445 19. Yagound B, Remnant EJ, Buchmann G, Oldroyd BP. Intergenerational transfer of DNA
446 methylation marks in the honey bee. *Proceedings of the National Academy of Sciences*.
447 2020;117(51):32519-27. pmid: 33257552
- 448 20. Wang X, Werren JH, Clark AG. Allele-specific transcriptome and methylome analysis reveals
449 stable inheritance and cis-regulation of DNA methylation in *Nasonia*. *PLoS biology*.
450 2016;14(7):e1002500. pmid: 27380029
- 451 21. Wang X, Li Q, Lian J, Li L, Jin L, Cai H, et al. Genome-wide and single-base resolution DNA
452 methylomes of the Pacific oyster *Crassostrea gigas* provide insight into the evolution of
453 invertebrate CpG methylation. *BMC Genomics*. 2014;15(1):1119. pmid: 25514978

- 454 22. Olson CE, Roberts SB. Genome-wide profiling of DNA methylation and gene expression in
455 *Crassostrea gigas* male gametes. *Frontiers in physiology*. 2014;5:224. pmid: 24987376.
- 456 23. Gavery MR, Roberts SB. Predominant intragenic methylation is associated with gene
457 expression characteristics in a bivalve mollusc. *PeerJ*. 2013;1:e215-e. pmid: 24282674.
- 458 24. Riviere G, He Y, Tecchio S, Crowell E, Gras M, Sourdain P, et al. Dynamics of DNA
459 methylomes underlie oyster development. *PLoS genetics*. 2017;13(6):e1006807. pmid:
460 28594821
- 461 25. Olson CE, Roberts SB. Indication of family-specific DNA methylation patterns in developing
462 oysters. *BioRxiv*. 2015:012831.
- 463 26. Wang X, Li A, Wang W, Que H, Zhang G, Li L. DNA methylation mediates differentiation in
464 thermal responses of Pacific oyster (*Crassostrea gigas*) derived from different tidal levels.
465 *Heredity*. 2021;126(1):10-22. pmid: 32807851
- 466 27. Wang X, Li A, Wang W, Zhang G, Li L. Direct and heritable effects of natural tidal
467 environments on DNA methylation in Pacific oysters (*Crassostrea gigas*). *Environmental*
468 *research*. 2021;197:111058. pmid: 33757824
- 469 28. Johnson KM, Kelly MW. Population epigenetic divergence exceeds genetic divergence in the
470 Eastern oyster *Crassostrea virginica* in the Northern Gulf of Mexico. *Evol Appl*. 2020;13:945 -
471 59. pmid: 32431745
- 472 29. Zemach A, McDaniel IE, Silva P, Zilberman D. Genome-Wide Evolutionary Analysis of
473 Eukaryotic DNA Methylation. *Science*. 2010;328(5980):916-9. pmid: 20395474
- 474 30. Weber M, Hellmann I, Stadler MB, Ramos L, Pääbo S, Rebhan M, et al. Distribution, silencing
475 potential and evolutionary impact of promoter DNA methylation in the human genome. *Nature*
476 *genetics*. 2007;39(4):457-66. pmid: 17334365

- 477 31. Sun D, Yu H, Li Q, DNA methylation differences between male and female gonads of the
478 oyster reveal the role of epigenetics in sex determination. *Gene*. 2021; Forthcoming
- 479 32. Sun D, Xi Y, Rodriguez B, Park HJ, Tong P, Meong M, et al. MOABS: model based analysis
480 of bisulfite sequencing data. *Genome Biology*. 2014;15(2):R38. pmid: 24565500
- 481 33. Jiang Q, Li Q, Yu H, Kong L. Inheritance and Variation of Genomic DNA Methylation in
482 Diploid and Triploid Pacific Oyster (*Crassostrea gigas*). *Mar Biotechnol (NY)*. 2016;18(1):124-
483 32. pmid: 26585587.
- 484 34. Tian T, Liu Y, Yan H, You Q, Yi X, Du Z, et al. agriGO v2.0: a GO analysis toolkit for the
485 agricultural community, 2017 update. *Nucleic Acids Research*. 2017;45(W1):W122-W9. pmid:
486 28472432
- 487 35. Hodge RG, Ridley AJ. Regulating Rho GTPases and their regulators. *Nature Reviews*
488 *Molecular Cell Biology*. 2016;17(8):496-510. pmid: 27301673
- 489 36. Law JA, Jacobsen SE. Establishing, maintaining and modifying DNA methylation patterns in
490 plants and animals. *Nature Reviews Genetics*. 2010;11(3):204-20. pmid: 20142834
- 491 37. Lee TF, Zhai J, Meyers BC. Conservation and divergence in eukaryotic DNA methylation.
492 *Proc Natl Acad Sci U S A*. 2010;107(20):9027-8. pmid: 20457928
- 493 38. Peñaloza C, Gutierrez AP, Eöry L, Wang S, Guo X, Archibald AL, et al. A chromosome-level
494 genome assembly for the Pacific oyster *Crassostrea gigas*. *GigaScience*. 2021;10(3). pmid:
495 33764468
- 496 39. Zhou W, Liang G, Molloy PL, Jones PA. DNA methylation enables transposable element-
497 driven genome expansion. *Proceedings of the National Academy of Sciences*.
498 2020;117(32):19359-66. pmid: 32719115

- 499 40. Stadler MB, Murr R, Burger L, Ivanek R, Lienert F, Schöler A, et al. DNA-binding factors
500 shape the mouse methylome at distal regulatory regions. *Nature*. 2011;480(7378):490-5. pmid:
501 22170606
- 502 41. Lister R, Pelizzola M, Dowen RH, Hawkins RD, Hon G, Tonti-Filippini J, et al. Human DNA
503 methylomes at base resolution show widespread epigenomic differences. *Nature*.
504 2009;462(7271):315-22. doi: 10.1038/nature08514.
- 505 42. Varley KE, Gertz J, Bowling KM, Parker SL, Reddy TE, Pauli-Behn F, et al. Dynamic DNA
506 methylation across diverse human cell lines and tissues. *Genome Res*. 2013;23(3):555-67. pmid:
507 23325432
- 508 43. Gelfman S, Cohen N, Yearim A, Ast G. DNA-methylation effect on cotranscriptional splicing
509 is dependent on GC architecture of the exon–intron structure. *Genome Res*. 2013;23(5):789-99.
510 pmid: 23502848
- 511 44. Shayevitch R, Askayo D, Keydar I, Ast G. The importance of DNA methylation of exons on
512 alternative splicing. *Rna*. 2018;24(10):1351-62. pmid: 30002084
- 513 45. Neri F, Rapelli S, Krepelova A, Incarnato D, Parlato C, Basile G, et al. Intragenic DNA
514 methylation prevents spurious transcription initiation. *Nature*. 2017;543(7643):72-7. pmid:
515 28225755
- 516 46. Skvortsova K, Tarbashevich K, Stehling M, Lister R, Irimia M, Raz E, et al. Retention of
517 paternal DNA methylome in the developing zebrafish germline. *Nature Communications*.
518 2019;10(1):3054. pmid: 31296860
- 519 47. Hall E, Volkov P, Dayeh T, Esguerra JLS, Salö S, Eliasson L, et al. Sex differences in the
520 genome-wide DNA methylation pattern and impact on gene expression, microRNA levels and

- 521 insulin secretion in human pancreatic islets. *Genome biology*. 2014;15(12):1-22. pmid:
522 25517766
- 523 48. Cisternas CD, Cortes LR, Bruggeman EC, Yao B, Forger NG. Developmental changes and sex
524 differences in DNA methylation and demethylation in hypothalamic regions of the mouse brain.
525 *Epigenetics*. 2020;15(1-2):72-84. pmid: 31378140
- 526 49. Landen S, Jacques M, Hiam D, Romero JA, Harvey NR, Haupt LM, et al. Genome-wide DNA
527 methylation and transcriptome integration reveal distinct sex differences in skeletal muscle.
528 bioRxiv: 435733v2. 2021 [cited 2021 December 22]. Available from:
529 <https://www.biorxiv.org/content/10.1101/2021.03.16.435733v2>
- 530 50. Puetz S, Lubomirov LT, Pfitzer G. Regulation of smooth muscle contraction by small GTPases.
531 *Physiology*. 2009;24(6):342-56. pmid: 19996365
- 532 51. Charrasse S, Causeret M, Comunale F, Bonet-Kerrache A, Gauthier-Rouvière C. Rho GTPases
533 and cadherin-based cell adhesion in skeletal muscle development. *Journal of Muscle Research
534 & Cell Motility*. 2003;24(4):311-5. pmid: 14620744
- 535 52. Chen S, Zhou Y, Chen Y, Gu J. fastp: an ultra-fast all-in-one FASTQ preprocessor.
536 *Bioinformatics*. 2018;34(17):i884-i90. pmid: 30423086
- 537 53. Xi Y, Li W. BSMAP: whole genome bisulfite sequence MAPping program. *BMC
538 Bioinformatics*. 2009;10:232. PubMed pmid: 19635165
- 539 54. Lin X, Sun D, Rodriguez B, Zhao Q, Sun H, Zhang Y, et al. BSeQC: quality control of bisulfite
540 sequencing experiments. *Bioinformatics*. 2013;29(24):3227-9. pmid: 24064417
- 541 55. Kim D, Paggi JM, Park C, Bennett C, Salzberg SL. Graph-based genome alignment and
542 genotyping with HISAT2 and HISAT-genotype. *Nature Biotechnology*. 2019;37(8):907-15.
543 pmid: 31375807

- 544 56. Putri GH, Anders S, Pyl PT, Pimanda JE, Zanini F. Analysing high-throughput sequencing
545 data in Python with HTSeq 2.0. arXiv:211200939 [Preprint]. 2021 [cited 2021 December 22].
546 Available from: <https://arxiv.org/abs/2112.00939>
- 547 57. Smit, AFA, Hubley, R & Green, P. RepeatMasker Open-4.0. 2013-2015. Available from:
548 <http://www.repeatmasker.org>
- 549 58. Smit, AFA, Hubley, R. RepeatModeler Open-1.0. 2008-2015. Available from:
550 <http://www.repeatmasker.org>
- 551 59. Jurka J, Kapitonov VV, Pavlicek A, Klonowski P, Kohany O, Walichiewicz J. Repbase Update,
552 a database of eukaryotic repetitive elements. Cytogenetic and genome research. 2005;110(1-
553 4):462-7. pmid: 16093699

554

555 **Supporting information**

556 **S1 Fig. Standard quality control of DNA methylation analysis in *C. gigas***

557 (A) Schematic of the experimental design. Two pairs of parents (n = 4), diploid oysters (n = 6) and
558 triploid oysters (n = 6), were used in this study. (B) The relationship between DNA methylation
559 levels and sequencing depth. And the relationship between coverage of CpG sites and sequencing
560 depth. (C) Pearson correlation analysis between WGBS data in this study and public WGBS data
561 of *C. gigas*. (D) DNA methylation levels across the gene body of all *C. gigas* samples analyzed in
562 this study. (E) Histograms of DNA methylation levels distributions for all analyzed samples. (F)
563 DNA methylation levels at the indicated regulatory elements in all analyzed samples. (G) The
564 relationship between DNA methylation levels and transcripts across the gene body in triploid
565 oyster samples.

566 **S2 Fig. DNA methylation differences between colonies, male and female, and diploid and**
567 **triploid oysters**

568 (A-B) The University of California, Santa Cruz (UCSC) genome browser view of DNA
569 methylation enrichment at the *DGKD* locus (NC_047562.1:45,716,336-45,757,148) in parent
570 cohort (A) and offspring cohort (B). The highlighted region exhibits decreased methylation in
571 females. (C) Heatmap of the DNA methylation levels in regulatory elements across all samples
572 analyzed in this study. (D) Heatmap of the Pearson correlation coefficient using pairwise common
573 CpGs methylation levels across all samples. (E) Histogram showing the numbers of hypo-DMCs
574 and hyper DMCs identified between colony one and two, males and females, diploid and triploid
575 oysters.

576 **S3 Fig. Differentially methylated genes between male and female in *C. gigas***

577 (A) Histogram showing the distribution of hypo-DMRs in chromosomes. (B) Histogram showing
578 the distribution of hypo-DMRs in regulatory elements. (C) The hierarchical structure and ancestry
579 relationships in the gene ontology top enriched terms. (D) UCSC genome browser view of DNA
580 methylation enrichment at the *FGDI* locus (NC_047566.1:24989612-25017157) (left) and *FGD6*
581 locus (NC_047566.1:21330721-21358510) (right) in all samples analyzed in this study. The
582 highlighted region by dotted line exhibits decreased methylation in females. (E) Boxplot shows
583 FPKM values of *FGDI* (left) and *FGD6* (right) in male and female groups in *C. gigas* ($P < 0.05$).

584 **S1 Table. Sample information and WGBS data statistics.**

585 16 samples collected from two independent families included parents and progenies. 2x75bp
586 paired-end sequencing was performed in this study. The results of WGBS data analysis included
587 numbers of filtered FASTQ reads (Total reads), unique mapped reads (Uniq mapped reads), unique
588 mapping ratio (Mapping ratio), bisulfite conversion efficiencies estimated from spike-in Lambda

589 genome (Bcr Lambda), bisulfite conversion efficiencies estimated from whole genome (Bcr whole
590 genome), CpG sites with at least 5 times coverage (Number of CpGs), effective reads ratio
591 (Positive rate), global CpGs methylation ratio (Mean ratio of CpGs).

592 **S2 Table. Results of gender determination across all samples analyzed in this study.**

593 Males included p8m, o8d_1, o8d_3, p10m, o10d_1, o10d_3. Females included p8f, o8d_2, o8t_1,
594 o8t_2, o8t_3, p10f, o10d_2, o10t_1, o10t_2, o10t_3.

595 **S3 Table. Regulation of Ras protein signal transduction process enriched in Gene ontology
596 analysis.**

597 In regulation of Ras protein signal transduction process significantly enriched in this study, 21
598 genes functioning as guanine nucleotide exchange factors (GEFs) were hypomethylated in *C. gigas*
599 females.

600

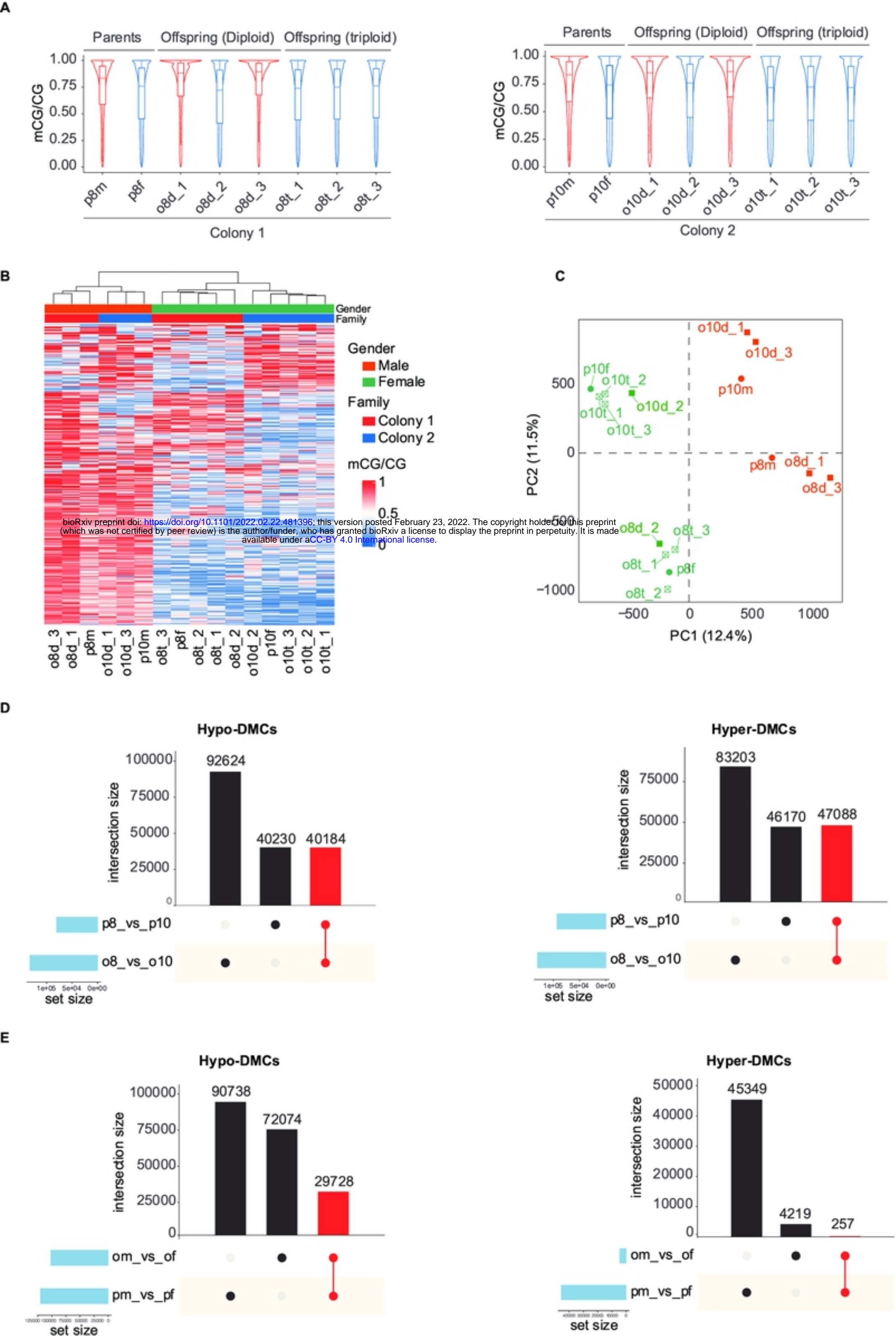


Fig2

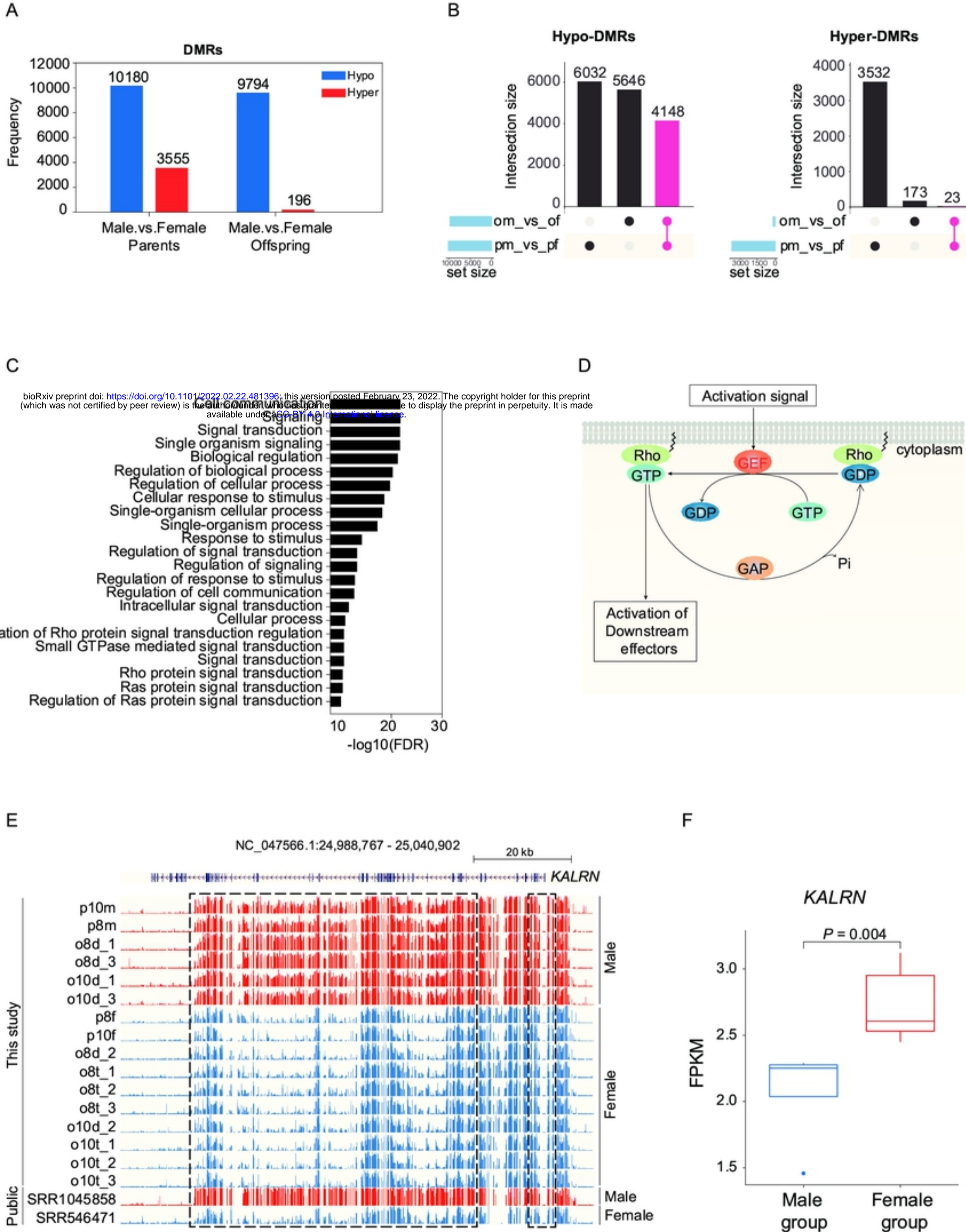
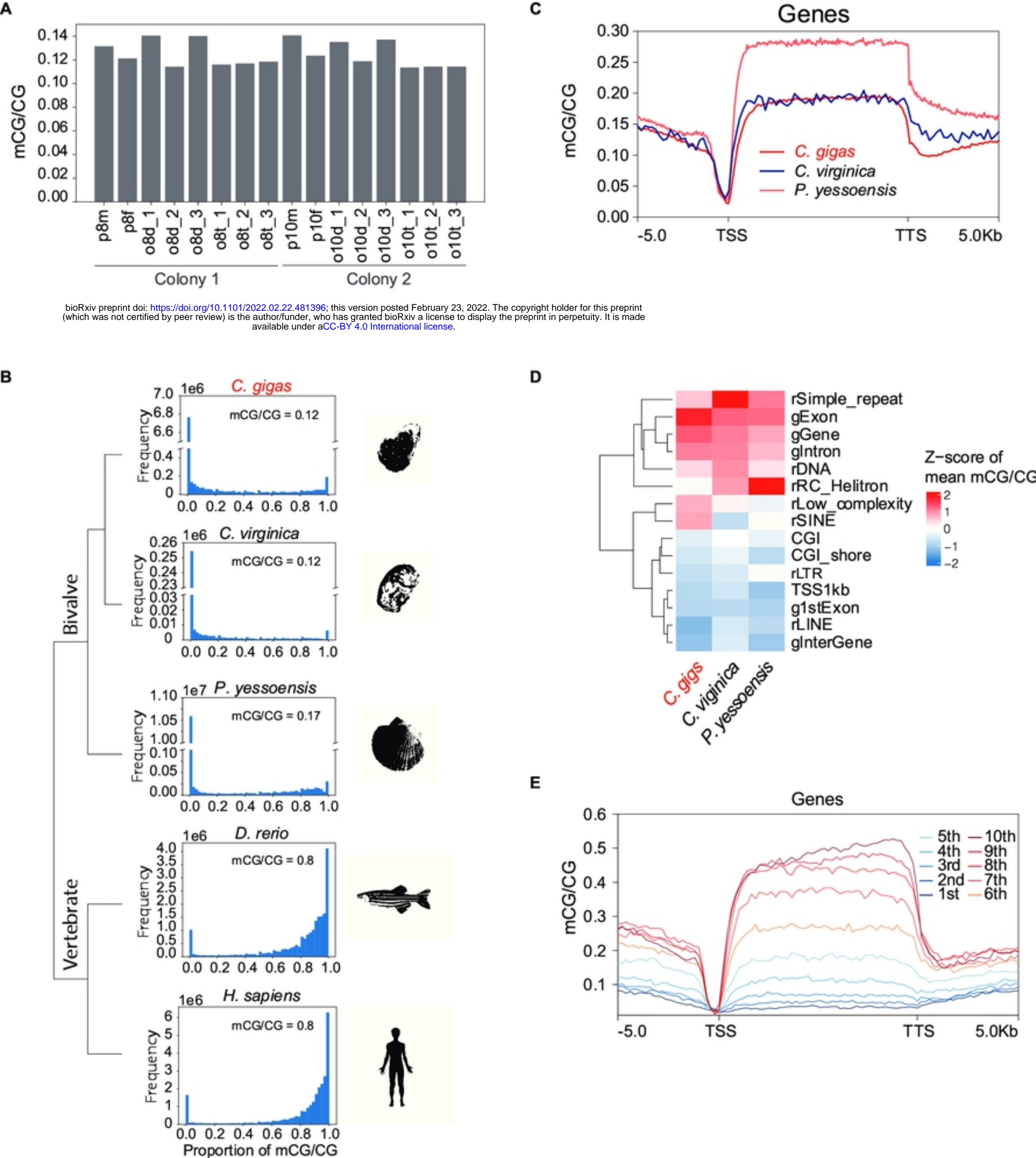


Fig3



bioRxiv preprint doi: <https://doi.org/10.1101/2022.02.22.481396>; this version posted February 23, 2022. The copyright holder for this preprint (which was not certified by peer review) is the author/funder, who has granted bioRxiv a license to display the preprint in perpetuity. It is made available under aCC-BY 4.0 International license.

Fig1